Star Formation in Dense Molecular Gas: The HCN-to-HCO$^+$ Ratio

Madisyn Brooks[1] and Amanda Kepley[2]

[1] *University of Central Florida, Orlando, FL 32816-2385, USA*
[2] *National Radio Astronomy Observatory, 520 Edgemont Road, Charlottesville, VA 22903, USA*

ABSTRACT

HCN(1-0) and HCO$^+$(1-0) can be used to study the dense parts of gas in molecular clouds. The HCN(1-0)/HCO$^+$(1-0) line ratio has been previously used to distinguish between starburst and AGN regions in galactic centers, however, as the galaxy samples increase, the HCN(1-0)/HCO$^+$(1-0) line ratio might present a more complicated picture of nuclear activity in galaxies. We present HCN(1-0) and HCO$^+$(1-0) integrated line flux measurements from the inner $2'$ by $2'$ of 16 nearby galaxies mapped from the Dense Extragalactic GBT+Argus Survey (DEGAS). We describe the methodology used to calculate the integrated line fluxes and study the relationship between the HCN(1-0)/HCO$^+$(1-0) line ratio and the total luminous infrared emission (LTIR). The HCN(1-0)/HCO$^+$(1-0) line ratios we calculated is consistent with samples in other galaxies. We looked at variations of the HCN(1-0)/HCO$^+$(1-0) line ratio along the spiral arms of 4 galaxies that showed distinct spiral arm features in our field of view. We find no definite HCN(1-0)/HCO$^+$(1-0) trend along the spiral arm regions and suggest HCN(1-0)/HCO$^+$(1-0) depends on local environmental conditions in the spiral arms. We suggest that barred and unbarred spirals show different HCN(1-0)/HCO$^+$(1-0) correlations with LTIR. Barred spirals show no trend with LTIR, while unbarred spirals show a positive trend with LTIR that is driven by two outlier galaxies. Also, with an analysis of the HCN(1-0)/HCO$^+$(1-0) line ratio across increasing aperture sizes, we determine that HCN(1-0)/HCO$^+$(1-0) does not change, omitting two outlier galaxies, across decreasing total infrared surface brightness.

1. INTRODUCTION

Most modern theories attribute gas density to be the main driver of star formation. Studies of star-forming regions performed in the Milky Way and nearby galaxies have observed a correlation between dense molecular gas and star formation (e.g. Lada & Lada 2003; Gao & Solomon 2004; Leroy et al. 2008; Heiderman et al. 2010; Bigiel et al. 2015). It is believed that CO(1-0) emissions trace the bulk of the molecular medium (Young & Scoville 1982) while emissions from molecules with higher dipole moments are used as a probe for dense gas in external galaxies. HCN(1-0) and HCO$^+$(1-0) have critical densities $\approx$ 3 x 10^6 cm^{-3} and $\approx$ 3 x 10^6 cm^{-3} respectively, at 30 K, which are factors of $\sim$ 100 higher than CO(1-0). HCN(1-0) and HCO$^+$(1-0) will be referred to as HCN and HCO$^+$ for the remainder of the paper. These high critical densities allow HCN and HCO$^+$ to be associated with higher density molecular hydrogen and therefore are useful for tracing the dense molecular gas associated with star formation (Gao & Solomon 2004).

The samples of studies involving dense gas have been limited due to the faint nature of molecular emissions from molecules like HCN and HCO$^+$ (Meier et al. 2015). However, modern instrumentation is now making the observations of faint molecular lines in nearby galaxies more accessible, due in part to their super sensitivity and high resolution. The Dense Extragalactic GBT+Argus Survey (DEGAS) utilizes the large aperture of the Green Bank Telescope (GBT) and the 16-pixel, 3mm focal plane array of Argus to conduct these ultra-sensitive molecular detections and to help further our understanding of the role dense gas plays in star formation. The goal of DEGAS is to quantify the relationship between gas dense and star formation and it works to accomplish this feat by mapping four dense gas tracers, ^{13}CO, C^{18}O, HCN, and HCO$^+$, in the inner $2'$ minutes by $2'$ of 36 galaxies.

This project is a subset of the overarching goal of DEGAS and focuses on the HCN/HCO$^+$ line ratio and its relationship with total infrared emission. Several studies of galaxy systems that host active galactic nuclei (AGNs) have found an enhanced HCN/HCO$^+$ line ratio when compared to the HCN/HCO$^+$ line ratio previously observed in starburst galaxies (Graciá-Carpio et al. 2006; Imanishi et al. 2007). These studies find a linear relationship between the HCN/HCO$^+$ line ratio and the total infrared emission. Galaxy systems containing an AGN tend to have higher total

infrared emissions than their starburst system counterparts, suggesting that the presence of an AGN should enhance the HCN/HCO$^+$ line ratio. Recent studies disagree with these findings and find no clear trend for the HCN/HCO$^+$ line ratio and the infrared luminosities (Privon et al. 2015, 2020; Li et al. 2021). These results present a more complicated picture of the parameters that affect the HCN/HCO$^+$ line ratio.

This paper presents the study conducted on the relationship between the HCN/HCO$^+$ line ratio and the total infrared emission using data collected from the DEGAS survey. The DEGAS sample of galaxies focuses on the central $2'$ by $2'$ of intermediate spiral-galaxies with a resolution of ~ 750 pc (with some outliers; e.g. NGC2146, NGC4038), while previous surveys studied the whole star-forming area of nearby massive spirals with a resolution of ~ 1.5 kpc (Jiménez-Donaire et al. 2019) and the inner 3 kpc of nearby galaxies with a resolution of ~ 200 pc (Gallagher et al. 2018). The DEGAS sample will help connect previous studies of star-forming clouds in the Milky Way with integrated measurements of whole galaxies by mapping dense gas tracers in nearby galaxies.

2. METHODOLOGY

HCN and HCO$^+$ spectral lines were mapped with the Green Bank Telescope (GBT) using the 16-pixel plane array Argus in 17 galaxies with a spectral resolution of 10 km s^{-1}. The integrated line flux for HCN and HCO$^+$ was calculated by finding the width of the spectral line and summing over the spectral channels included in the line. A single-profile Gaussian was fitted to the spectral lines and the width of the spectral line was then determined by using the peak of the Gaussian profile of the brighter line and 2σ on either side of the peak. Figure 1 gives an example of the HCN and HCO+ spectral lines and their corresponding Gaussian fit.

The errors on the spectral lines were calculated using the standard deviation of the line in the parts of the spectrums that contained no signal. A non detection of either of the molecules is defined when the measured line is less than three times the calculated error. HCO$^+$ was not detected for NGC3147 and HCN was not detected for NGC3521. Neither of the molecules were detected for NGC0337. 3σ upper limits were computed where the emission lines are undetected, these limits were computed as:

$$3\sigma_{rms} \times \Delta v_{chan} \times \sqrt{n_{chan}} \tag{1}$$

where $\sigma_{\rm rms}$ is the 1σ rms value of the noise in K, which is measured from the part of the spectrum that is signal free, Δv_{chan} is the width of each channel in km s^{-1}, and n_{chan} is the number of channels included in the integrated flux line measurement derived from the Gaussian fit.

Three different analyses were conducted using the HCN/HCO$^+$ line ratio. The first analysis was done by measuring the total luminous infrared emission in the inner $30''$ of the galaxies with detections of both molecules. Figure 2 shows an example of the inner $30''$ region of a galaxy. The total luminous infrared emission for the inner $30''$ of the galaxies' centers was calculated using the following:

$$L_{TIR} = \pi \times (\mathrm{d} \times \mathrm{r} \times 4.848 \times 10^{-6})^2 \times \frac{L_\odot}{pc^2} \tag{2}$$

where d is the distance to the galaxy in parsecs, r is the radius of the selected region, 4.848×10^{-6} is the arcseconds to radians conversion, and $\frac{L_\odot}{pc^2}$ is the mean infrared surface brightness of the selected region. The inner $30''$ of the galaxies was chosen as a means of comparison because intrinsically each galaxy has a different total infrared luminosity. This allows us to compare the HCN/HCO$^+$ line ratio from galaxy to galaxy and to determine if any trend is correlated with the LTIR. This also allows for the galaxies to be investigated based on morphology to determine if the structure of the galaxy can influence the HCN/HCO$^+$ line ratio.

The second analysis completed using the HCN/HCO$^+$ line ratio was performed in 4 galaxies which had distinct spiral arm features in our field of view. The 4 galaxies this analysis was completed for are: NGC2903, NGC3631, NGC4321, and NGC4535. The HCN/HCO$^+$ line ratio was measured in 7 $15''$ regions that extended from the galaxy's respective center and outwards along one of its distinct spiral arms. Figure 3 shows an example of the spiral arm regions extending from the center of a galaxy and outwards.

The third analysis completed using the HCN/HCO$^+$ line ratio was completed for all galaxies that had a detection of at least one of the molecules. The HCN/HCO$^+$ line ratio was measured using the inner $30''$ at the galaxy's center like the previous analysis, but the aperture of the measurement region was increased by $30''$ until the aperture reached $150''$. Figure 4 shows an example of a galaxy with increasing aperture region selections.
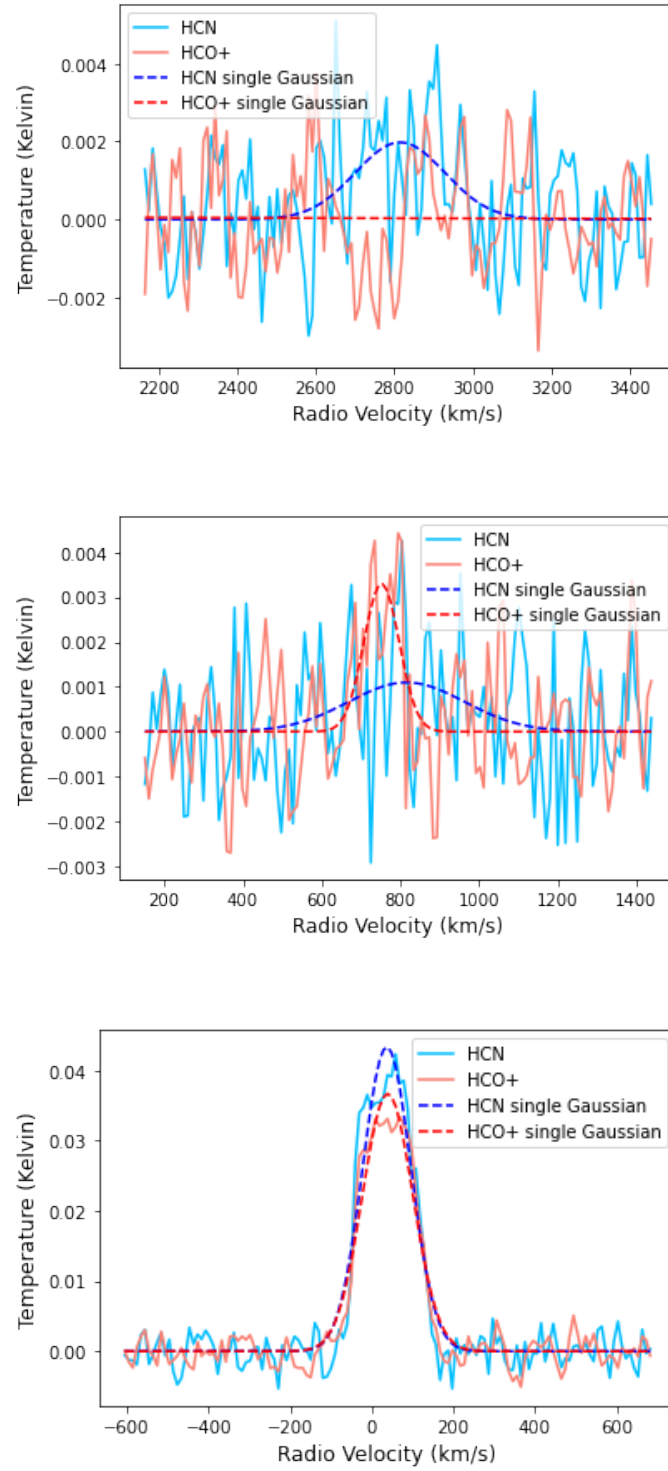
Figure 1. Spectral lines of HCN and HCO$^+$ for galaxies NGC3147 (top), NGC3521 (middle), and NGC6946 (bottom). Both lines are fitted with a single order Gaussian to determine the width of the spectral line. A non-detection for HCO$^+$ was found in NGC3147 and a non-detection for HCN was found in NGC3521.
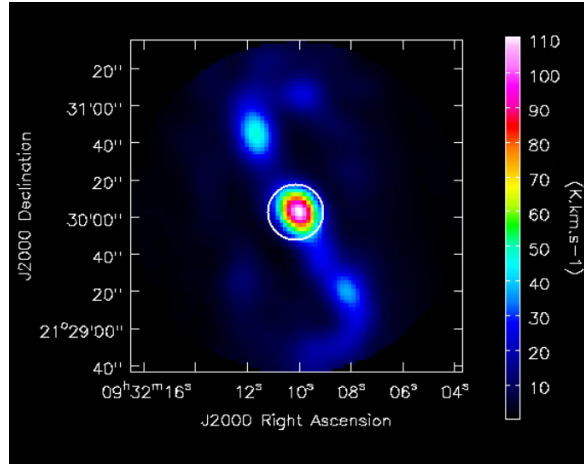
Figure 2. Inner 30″ (white) of galaxy NGC2903 plotted over the integrated intensity map of ^{12}CO.
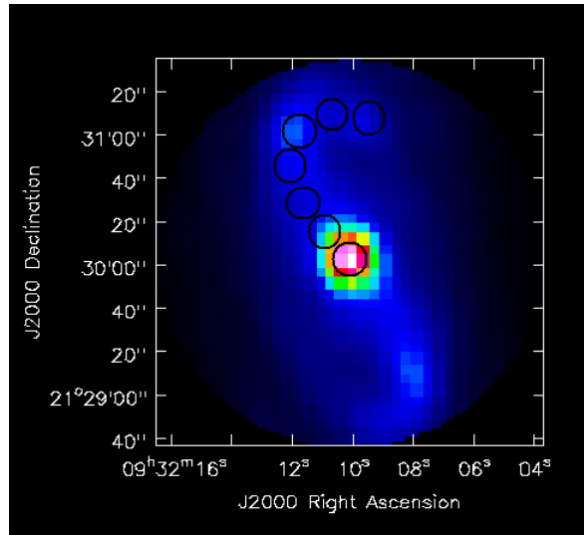
Figure 3. 7, 15″ regions (black) extending from the center and outward along the spiral arm of NGC2903 plotted over the map of stellar mass.

3. RESULTS

Table 1 shows the intergrated line fluxes calaculated for each galaxy and figure 5 shows a histogram of previous HCN/HCO$^+$ measures in comparison with HCN/HCO$^+$ computed from the new DEGAS data using the inner 30″ measurements. Our measurements are consistent with Privon et al. (2015) , who looked at galaxies similar to the DEGAS sample. We find HCN/HCO$^+$ that range from ~ 0.43 to ~ 4.1 with an average value of $\sim 1.55 \pm 0.1$. Privon et al. (2015) finds in AGN dominated systems a HCN/HCO$^+$ ratio of 1.84 ± 0.43, in Starburst dominated systems a ratio of 0.88 ± 0.28, while composite systems (both AGNs and Starbursts) have a ratio of 1.14 ± 0.49. Jiménez-Donaire et al. (2019) finds an average HCN/HCO$^+$ ratio of ~ 1.25.

We looked at how the morphology of the individual galaxies could affect the HCN/HCO$^+$ line ratio. In figure 6 we show that barred spiral galaxies show no dependence on the LTIR. This is consistent with Privon et al. (2015) and Li et al. (2021). While unbarred spiral galaxies have a slightly positive trend. These results are similar to what was reported in Graciá-Carpio et al. (2006) and Imanishi et al. (2007). It is important to note that NGC4414 (HCN/HCO$^+$ ≈ 4.11) and NGC4501 (HCN/HCO$^+$ ≈ 3.53) are driving this trend to be positive. NGC4501 has a documented AGN (Ho et al. 1997). which could be a possible explanation for the enhanced HCN line flux relative to HCO$^+$. NGC4414 is documented as a high density and gas rich galaxy with a possible bright nuclear source (Braine et al. 1997; Eskridge
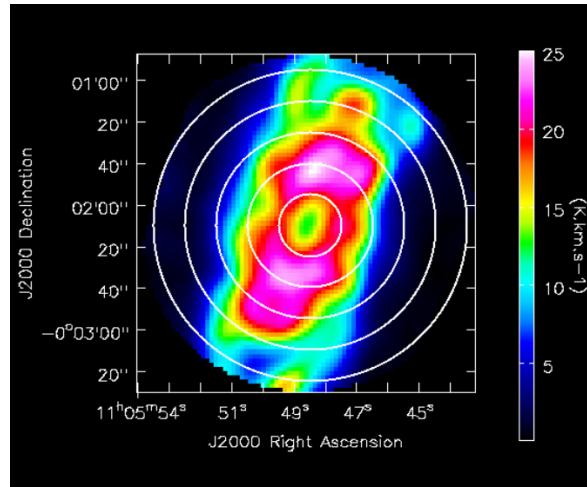
Figure 4. Increasing aperture in $30''$ increments, starting at $30''$ and increasing till $150''$ (white) of NGC3521 plotted over the integrated intensity map of ^{12}CO.

Table 1. Integrated line flux measurements using the inner 30 arc seconds of the DEGAS galaxy sample.

NAME	DISTANCE	MORPH	HCN	HCO$^+$
	(Mpc)		K km s^{-1}	K km s^{-1}
IC0342	2.99	SABc	6.17 ±0.42	5.12 ±0.36
NGC0337	19.5	SBcd		
NGC2146	22.1	SBab	5.22 ±0.11	4.38 ±0.08
NGC2903	8.47	Sbc	1.32 ±0.07	1.16 ±0.07
NGC3147	39.8	Sbc	0.57 ±0.08	<0.25
NGC3521	11.19	SABb	<0.12	0.29 ±0.04
NGC3631	18.0	Sc	0.34 ±0.03	0.10 ±0.03
NGC4030	19.0	Sbc	0.33 ±0.04	0.14 ±0.03
NGC4038	22.0	SBm	1.33 ±0.08	1.31 ±0.08
NGC4258	7.61	Sbc	0.98 ±0.10	1.62 ±0.07
NGC4321	15.2	SABb	2.08 ±0.10	1.54 ±0.07
NGC4414	17.7	Sc	1.24 ±0.09	0.30 ±0.08
NGC4501	16.8	Sb	1.14 ±0.09	0.32 ±0.05
NGC4535	15.8	Sc	0.58 ±0.06	0.50 ±0.05
NGC4569	16.8	Sab	1.36 ±0.08	1.69 ±0.07
NGC5055	8.87	Sbc	0.91 ±0.09	1.06 ±0.10
NGC6946	7.72	SABc	5.30 ±0.23	4.57 ±0.19

et al. 2002). The exclusion of these two galaxies would produce a fit line similar to that of the barred spirals. The trend for all galaxies has a slope of -0.292 ± 0.328.

Figure 7 shows the HCN/HCO$^+$ line ratio along the spiral arms of 4 different galaxies: NGC2903, NGC3631, NGC4321, and NGC4535. No consistent trend is seen along the arms of the 4 galaxies and suggests local conditions are affecting the line ratio in the individual galaxies. Also, the HCN/HCO$^+$ line ratio differs from arm region to arm region in individual galaxies, differing from an expected consistent ratio along the whole of the spiral arm.
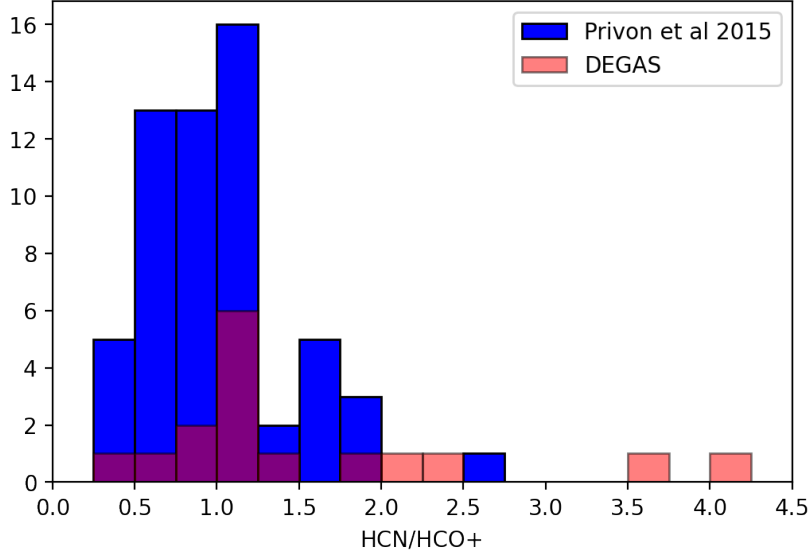
Figure 5. Comparison of the HCN/HCO$^+$ found by Privon et al 2015 (blue) and the current DEGAS sample (red).
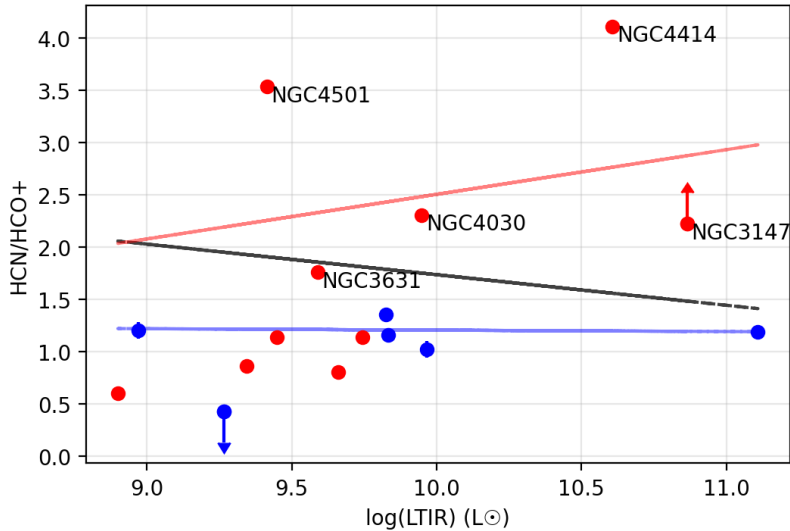
Figure 6. The HCN/HCO$^+$ was calculated for the inner 30 arc seconds of each galaxy and plotted against the log of the total infrared luminosity. Barred spiral galaxies (blue) show a slope of -0.013 $\pm$ .062 and unbarred spiral galaxies (red) show a slope of 0.427 $\pm$ 0.733. A fit line for both barred and unbarred galaxies (black) shows a slope of -0.292 $\pm$ 0.328. Galaxies with an HCN/HCO$^+$ line ratio > 1.5 are labeled as shown.

Figure 8 shows the final analysis completed for this study by a comparison of increasing aperture across all the galaxies. Increasing the region size of the HCN/HCO$^+$ line ratio decreases the average total infrared surface brightness. This allows for another comparison of the total infrared brightness versus the HCN/HCO$^+$ line ratio. If a dependence existed between the two, then a change in the HCN/HCO$^+$ line ratio would be seen with increasing aperture. The majority of the galaxies, except for outliers NGC3147 and NGC3521, show a flat trend across increasing aperture. NGC3147 contains an AGN (Bianchi et al. 2012) and NGC3521 contains an HII LINER (Low Ionization Nuclear Emission Region) (Das et al. 2003). Omitting these two galaxies, there is no trend with HCN/HCO$^+$ across increasing aperture.

4. SUMMARY AND CONCLUSIONS
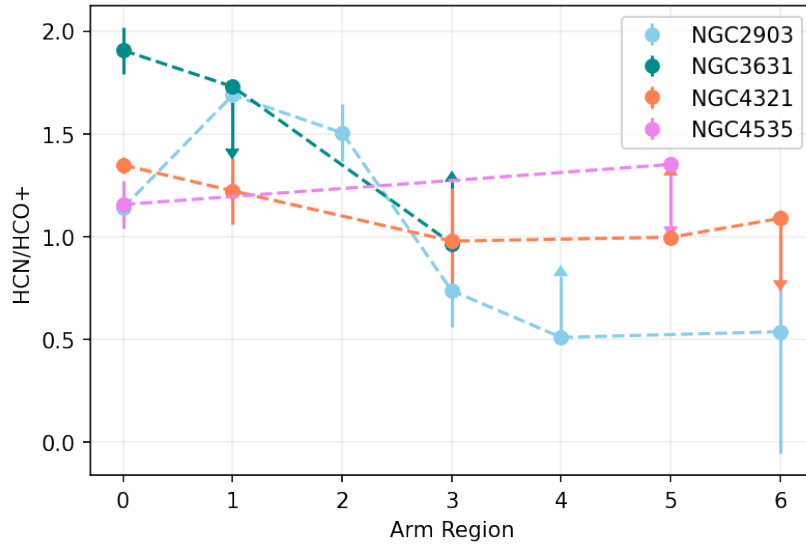
Figure 7. The HCN/HCO$^+$ for arm regions, $15''$ in diameter, 0 - 6 extending out from the galaxy's center (arm region 0) and out along the galaxy's respective spiral arm.
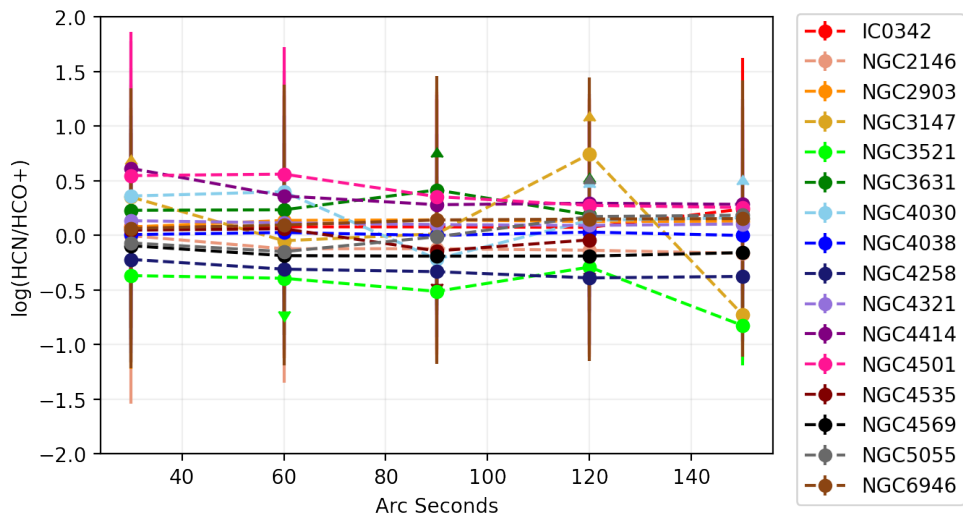
Figure 8. The HCN/HCO$^+$ for increasing aperture of $30''$ extending out from the galaxy's center.

The goal of DEGAS is to quantify the relationship between dense gas and star formation in nearby galaxies. The purpose of this study was to understand how HCN and HCO$^+$, two molecules tracing slightly different densities of gas, behaved across a sample of 17 intermediate star-forming spiral galaxies. Investigating the role of dense gas tracers HCN and HCO$^+$ allow for a deeper understanding of the physical mechanisms that drive star formation, help determine the affect that AGNs and other active nuclear environments have on the HCN/HCO$^+$ line ratio, and investigate the role of the HCN/HCO$^+$ line ratio as a diagnostic tool for AGNs. We present results of HCN and HCO$^+$ integrated line flux measurements for intermediate spiral galaxies mapped by DEGAS. Here we also describe the conclusions drawn from the anaylsis of the HCN/ HCO$^+$ line ratio:

1. Emissions from the dense gas tracers, HCN and HCO$^+$, were observed in 16 galaxies of the current DEGAS sample.

2. The HCN/HCO$^+$ line ratio on average for DEGAS galaxies is $\sim 1.55 \pm 0.1$

3. Barred and unbarred spirals show different trends with LTIR; barred spirals have no trend and unbarred spirals have a possible positive trend which is driven by two outlier galaxies, NGC4501 (AGN) and NGC4414 (bright nuclear source).

4. Local galactic conditions drive variations in the HCN/HCO^+ ratio along spiral arms when compared by galaxy; HCN/HCO^+ also varies in regions in individual spiral arms.

5. The HCN/HCO^+ ratio does not change, excluding outlier galaxies NGC3147 and NGC3521, with decreasing total infrared surface brightness

REFERENCES

Bianchi, S., Panessa, F., Barcons, X., et al. 2012, MNRAS, 426, 3225, doi: 10.1111/j.1365-2966.2012.21959.x

Bigiel, F., Leroy, A. K., Blitz, L., et al. 2015, ApJ, 815, 103, doi: 10.1088/0004-637X/815/2/103

Braine, J., Brouillet, N., & Baudry, A. 1997, A&A, 318, 19

Das, M., Teuben, P. J., Vogel, S. N., et al. 2003, ApJ, 582, 190, doi: 10.1086/344480

Eskridge, P. B., Frogel, J. A., Pogge, R. W., et al. 2002, ApJS, 143, 73, doi: 10.1086/342340

Gallagher, M. J., Leroy, A. K., Bigiel, F., et al. 2018, ApJ, 858, 90, doi: 10.3847/1538-4357/aabad8

Gao, Y., & Solomon, P. M. 2004, ApJ, 606, 271, doi: 10.1086/382999

Graciá-Carpio, J., García-Burillo, S., Planesas, P., & Colina, L. 2006, ApJL, 640, L135, doi: 10.1086/503361

Heiderman, A., Evans, Neal J., I., Allen, L. E., Huard, T., & Heyer, M. 2010, ApJ, 723, 1019, doi: 10.1088/0004-637X/723/2/1019

Ho, L. C., Filippenko, A. V., Sargent, W. L. W., & Peng, C. Y. 1997, ApJS, 112, 391, doi: 10.1086/313042

Imanishi, M., Nakanishi, K., Tamura, Y., Oi, N., & Kohno, K. 2007, AJ, 134, 2366, doi: 10.1086/523598

Jiménez-Donaire, M. J., Bigiel, F., Leroy, A. K., et al. 2019, ApJ, 880, 127, doi: 10.3847/1538-4357/ab2b95

Lada, C. J., & Lada, E. A. 2003, ARA&A, 41, 57, doi: 10.1146/annurev.astro.41.011802.094844

Leroy, A. K., Walter, F., Brinks, E., et al. 2008, AJ, 136, 2782, doi: 10.1088/0004-6256/136/6/2782

Li, F., Wang, J., Gao, F., et al. 2021, MNRAS, 503, 4508, doi: 10.1093/mnras/stab745

Meier, D. S., Walter, F., Bolatto, A. D., et al. 2015, ApJ, 801, 63, doi: 10.1088/0004-637X/801/1/63

Privon, G. C., Herrero-Illana, R., Evans, A. S., et al. 2015, ApJ, 814, 39, doi: 10.1088/0004-637X/814/1/39

Privon, G. C., Ricci, C., Aalto, S., et al. 2020, ApJ, 893, 149, doi: 10.3847/1538-4357/ab8015

Young, J. S., & Scoville, N. 1982, ApJL, 260, L11, doi: 10.1086/183860